A New Representation of the Single-Scattering Properties for Mid-latitude Clouds and its Impacts

G.M. McFarquhar, M.S. Timlin, and T. Nousiainen
University of Illinois
Department of Atmospheric Sciences
Urbana, Illinois

P. Yang
Texas A&M University
College Station, Texas

Introduction

McFarquhar et al. (2002) developed a parameterization for the single-scattering properties of tropical clouds and McFarquhar et al. (2003) found that both the representation of cloud microphysical and single-scattering properties affect estimates of cloud radiative forcing for single column model (SCM) simulations over the ARM TWP site. Thus it is important to explore how representations of microphysics and single-scattering properties vary for clouds forming in different geographical locations and associated with different formation mechanisms. Here, we combine state-of-the- art libraries of single scattering properties for idealized crystals with in-situ measurements of ice crystal number concentrations derived from standard optical array probes and with size-dependent habit distributions determined from the cloud particle imager (CPI) during the 2000 Cloud IOP to develop similar parameterizations for mid-latitude clouds. We also examine differences from the parameterizations developed for tropical clouds.

Shapes of Ice Crystals

During the 2000 Cloud IOP, small ice crystals were imaged with the Cloud Particle Imager (CPI) at 2.3 μm resolution during spiral descents of the University of North Dakota Citation over the SGP site through cirrus between -50 and -15°C. Figure 1 shows examples of these small crystals, most of which have a "quasi-spherical" shape. Given their variability and complex shapes, no simple function exists to describe their shapes. Nousiainen and McFarquhar (2004) used the Gaussian random sphere geometry (Figure 2) to describe these shapes, deriving the covariance of logradius from analysis of approximately 1000 CPI images.

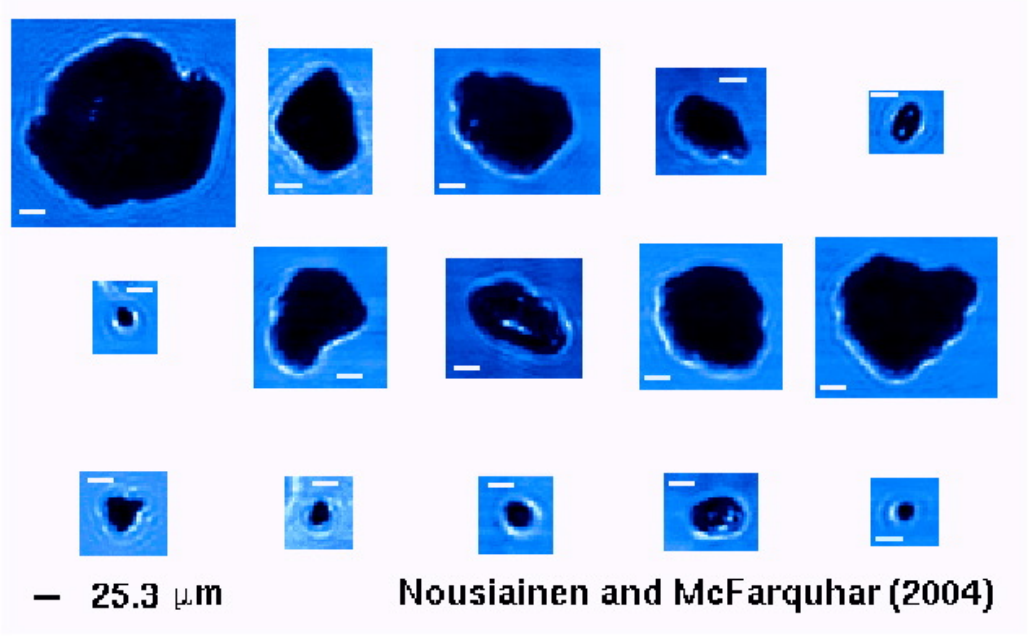

Figure 1. Quasi-spherical small crystals imaged by CPI during 2000 Cloud IOP.

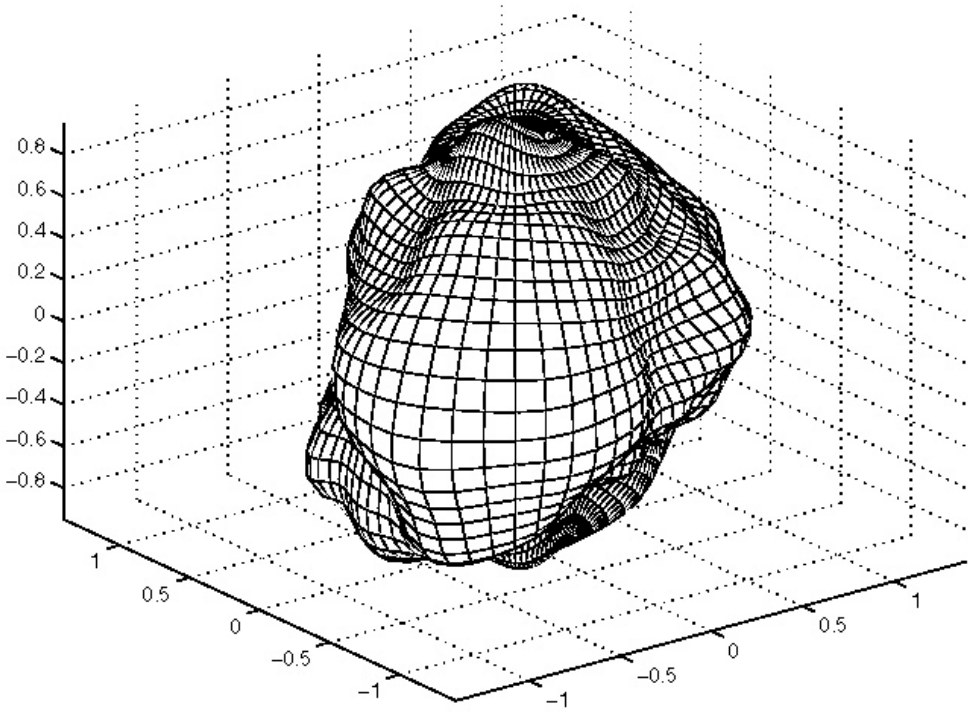

Figure 2. Example of random sphere geometry generated using shape statistics generated from analysis of CPI images.

These quasi-spheres are mixed with larger crystals, which have more pristine shapes (Figure 3). Their shapes vary from a preponderance of bullet rosettes on March 9, 2000 to a dominance of aggregates on March 12, 2000. Various measures of crystal morphology, such as maximum dimension, projected area, and perimeter are automatically generated by Stratton Park Engineering Company Inc.'s processing program CPIView. Relationships between these morphological features were analyzed for a number of crystals whose habits were manually identified in order to develop a habit identification scheme that could be applied to all crystals. The habit identification scheme in Figure 4 is applied to measures of crystal morphology calculated from CPIView in order to determine the size-dependent percentage of different habits for one-minute averaging periods. Although this averaging period is less than the averaging period for the size distributions measured by the optical array probes, the one-minute averaging period cannot be reduced because of the CPI's small sample volume. These percentages, combined with number distribution functions derived from the two-dimensional cloud probe (2DC) give the size and habit distributions (Figure 5). For crystals with $D < 120$ μm, number concentrations are calculated from the forward scattering spectrometer probe FSSP (5-50 μm) and the one-dimensional cloud probe 1DC (50-120 μm) and are assumed to be quasi- spheres.

The mass content can be computed from the size and shape distributions by making assumptions about how the mass or effective density of particles varies with particle dimension and area ratio (e.g., Mitchell 1996; Heymsfield et al. 2002). This mass content is then compared with that directly measured by the counterflow virtual impactor (CVI). Figure 6 shows that the CPI/2DC habit identification scheme provides good agreement with the total mass measured by the CVI. There is uncertainty in estimating number concentrations of small crystals having $D < 100$ μm. If we assume that the FSSP accurately measures small crystals, likely an overestimate, small crystals contribute less than 20% to total mass (Figure 7). Within the accuracy of mass calculations, the existence of these small crystals cannot be excluded. These small crystals can make non-negligible contributions to the cloud radiative properties.

Scattering Properties of Idealized Crystals

The mean single-scattering properties (asymmetry parameter g, single-scatter albedo ω_0 and extinction efficiency Q_{ext}) of crystal size/shape distributions are computed using observed size/ shape distributions and libraries of scattering properties for idealized crystals following McFarquhar et al. (2002). For $D > 120$ μm, this library is based on Yang's et al. (2000) improved geometric ray-tracing method for the habit classes identified by the CPI (aggregates, bullet rosettes, columns, plates and dendrites). For the Gaussian random spheres with $D < 120$ μm, size parameters x range from 3.2 to 1600 for $0.225\ \mu m < \lambda < 4.7\ \mu m$ implying different techniques are needed for small and large x. The discrete dipole approximation (e.g., Draine and Flatau 1994) is used for $x < 20$ and ray optics for $x > 50$. For $20 < x < 50$, interpolating between the 2 schemes for g and ω_0 gave better results than using simulations of simplified shapes. For Q_{ext}, since it approaches 2 asymptotically, it is interpolated from x=20 to 200 where ray optics is considered to be a good approximation.

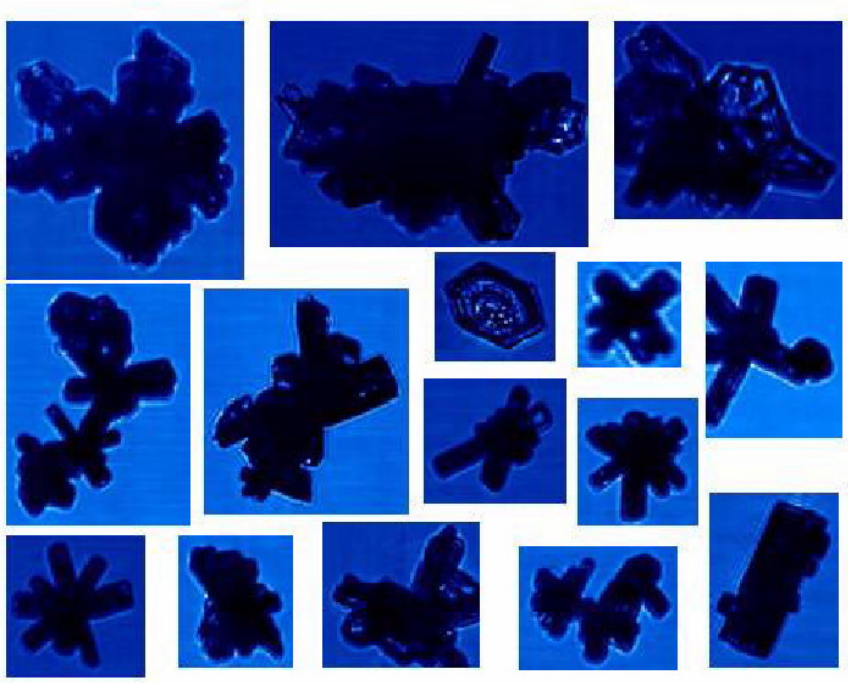

Figure 3. Examples of larger pristine crystals imaged by CPI during the 2000 spiral descents over the SGP.

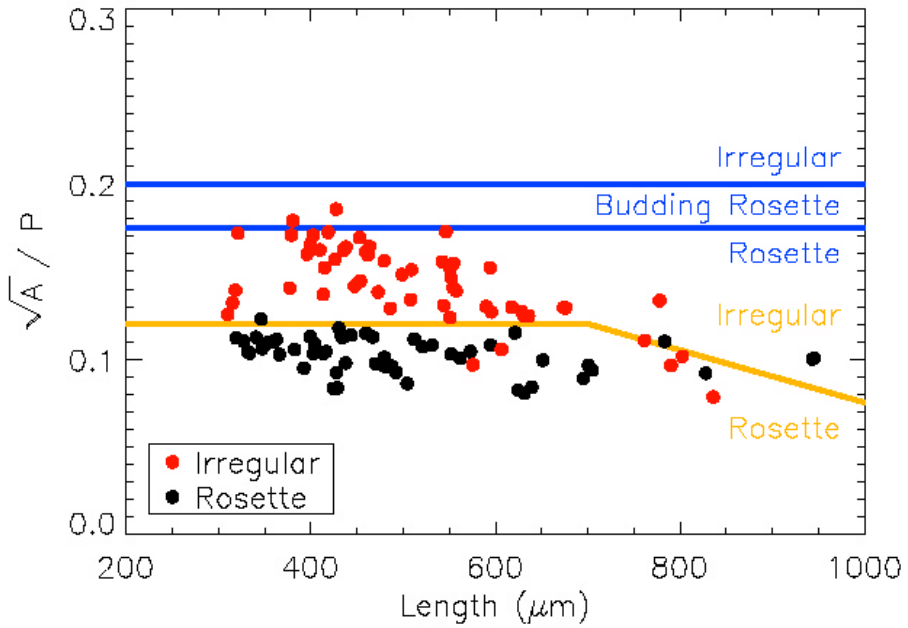

Figure 4. Relationship between length, cross-sectional area (A) and perimeter length (P) for a number of manually identified crystals. In this classification, irregular corresponds to aggregates. Yellow line represents habit identification scheme developed from these manually identified crystals, blue represents habit identification scheme supplied by SPEC based on analysis of images of crystals from Antarctic.

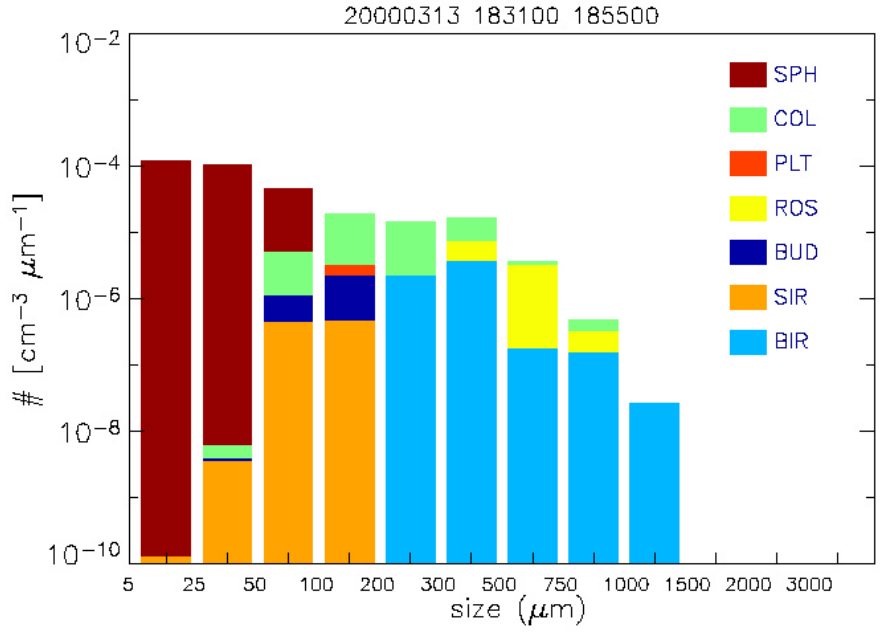

Figure 5. Example size and shape distributions for the March 13 spiral descent during the 2000 Cloud IOP determined from the CPI/2DC for D > 120 μm, and 1DC/FSSP for D < 120 μm.

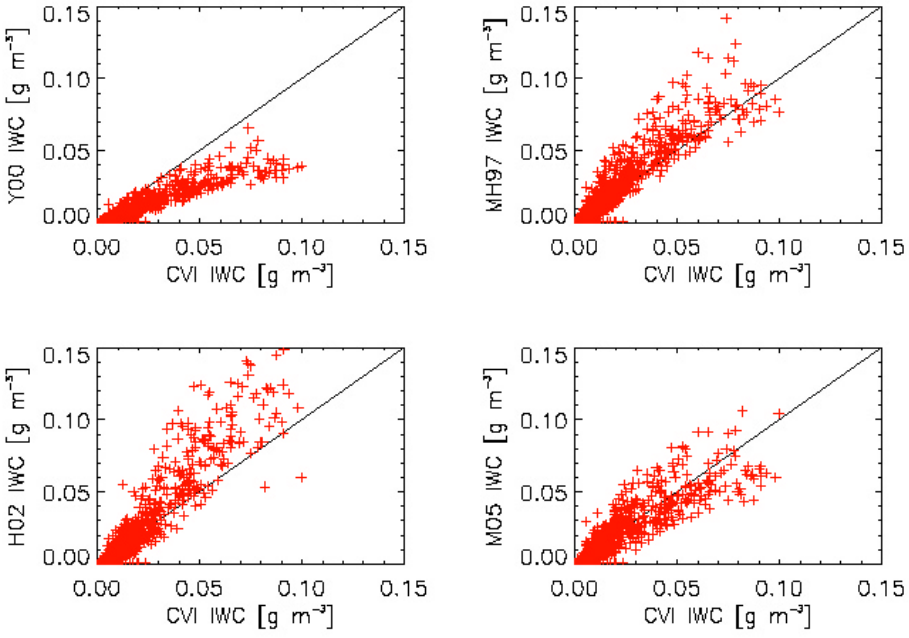

Figure 6. Comparison of bulk mass content measured by CVI against that estimated from 2DC or CPI/2DC size distributions and a variety of mass-diameter or mass-diameter-area ratio relationships. Y00 denotes masses from Yang et al. (2000) idealized crystals; MH97 habit identification and mass relationships of McFarquhar and Heymsfield (1997); H02 Heymsfield et al. (2002) mass relationships; and M05 McFarquhar et al. (2005) habit identification scheme using CPI data and 2DC size distributions.

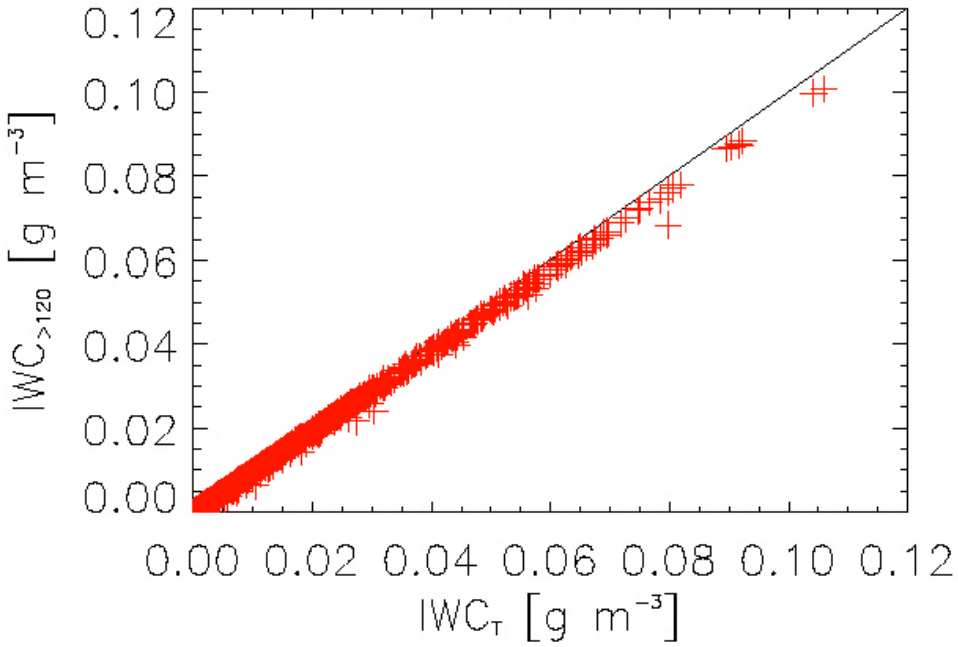

Figure 7. Mass estimated from 2DC/CPI size/habit distributions against mass estimated from 2DC/CPI plus that using the 1DC and FSSP size distributions. Small crystals from 1DC and FSSP contribute minimally to total mass.

Bulk Scattering Properties

Using the size and shape distributions derived from the CPI/2DC/FSSP/1DC data, the mean scattering properties are calculated for mid-latitudes representing the SGP site from the 2000 Cloud IOP data. Differences from those properties computed from the tropical clouds are noted and occur due to differences in habit distributions (more bullet rosettes in mid-latitudes), small crystal numbers (more small crystals in tropical anvils) and representations of small crystal shapes (Gaussian random spheres used here have a lower g than Chebyshev particles assumed in our tropical studies).

Summary

Analysis of more in-situ data is required to better characterize differences in sizes, shapes and numbers of small crystals in different geographic regimes and produced by different formation mechanisms. Data to be collected during TWP-ICE, where monsoonal, break-type convection and generic cirrus will be sampled with a similar suite of instruments used here, should help us further understand the differences between mid-latitude and tropical clouds.

Contact

M.S. Timlin, lin@atmos.uiuc.edu,

Acknowledgments

This research was supported by DOE ARM program under contract number DE-FG03- 00ER62913, Wanda Ferrell program manager. Data were obtained from the ARM archive sponsored by the U.S. Department of Energy, Office of Science, Office of Biological and Environmental Research, Environmental Sciences Division.

References

Draine and Flatau 4

Fu, Q. 1996. "An accurate parameterization of the solar radiative properties of cirrus clouds for climate models." *J. Climate* 9, 2058-2082.

Heymsfield et 2002. "A general approach for deriving the properties of cirrus and stratiform ice cloud particles." *J. Atmos. Sci.* 59, 3-29.

McFarquhar, GM, and AJ Heymsfield. 1997. "Parameterization of tropical cirrus ice crystal size distributions and implications for radiative transfer: Results from CEPEX." *J. Atmos. Sci.* 54, 2187-2200.

McFarquhar, GM, P Yang, A Macke, and AJ Baran. 2002. "A new parameterization of single scattering solar radiative properties for tropical anvils using observed ice crystal size and shape distributions." *J. Atmos. Sci*. 59, 2458-2478.

McFarquhar, GM, S Iacobellis, and RCJ Somerville. 2003. "SCM simulations of tropical ice clouds using observationally based parameterizations of microphysics." *J. Climate* 16, 1643-1664.

McFarquhar, GM, MS Timlin, and T Nousiainen. 2005. "A new representation of the mean scattering properties of mid-latitude cirrus and its impacts." *J. Atmos. Sci.* (To be submitted.)

Mitchell, DL. 1996. "Use of mass- and area-dimensional power laws for determining precipitation particle terminal velocities." *J. Atmos. Sci.* 53, 1710-1723.

Nousiainen and McFarquhar (4)

Vogelman, AM, and TP Ackerman. 1995. "Relating cirrus cloud properties to observed fluxes: A critical assessment." *J. Atmos. Sci.* 52, 4285-4301.

Yang, P, KN Liou, K Wyser, and D Mitchell. 2000. "Parameterization of the scattering and absorption properties of individual ice crystals." *J. Geophys. Res.* 105, 4699-4718.

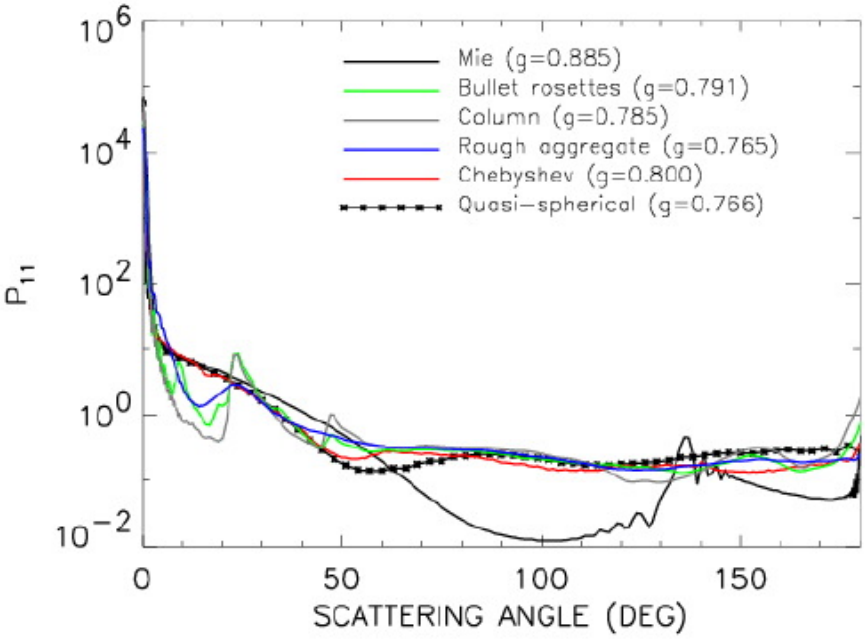

Figure 8. Scattering phase function at λ=0.55 μm for variety of shapes with D = 60 μm. Differences between g are significant for representation of single-scattering properties in large-scale models given needed accuracy of between 2 and 5% in radiative fluxes (Vogelman and Ackerman 1995).

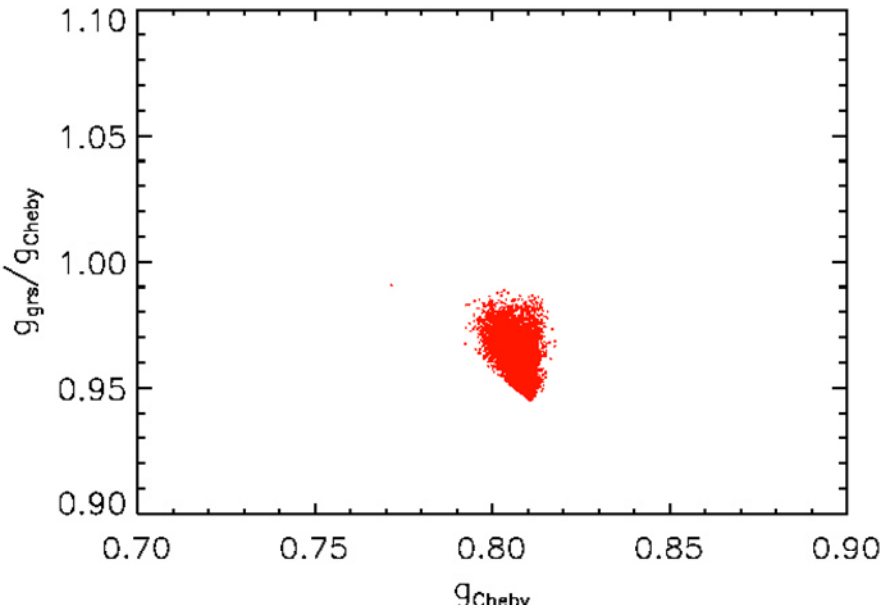

Figure 9. Plot of g_{rs}/g_{Cheby} as function of g_{Cheby} for 0.25 < λ < 0.69 μm, where g_{rs} represents mean g calculated assuming random sphere geometry for small crystals and g_{Cheby} calculated assuming expansions of quasi-sphere geometry in terms of Chebyshev polynomials for small crystals (size distributions from Tropics and should be representative of conditions at TWP site). Difference shows that must carefully consider representation of small crystal shapes when calculating single-scattering properties.

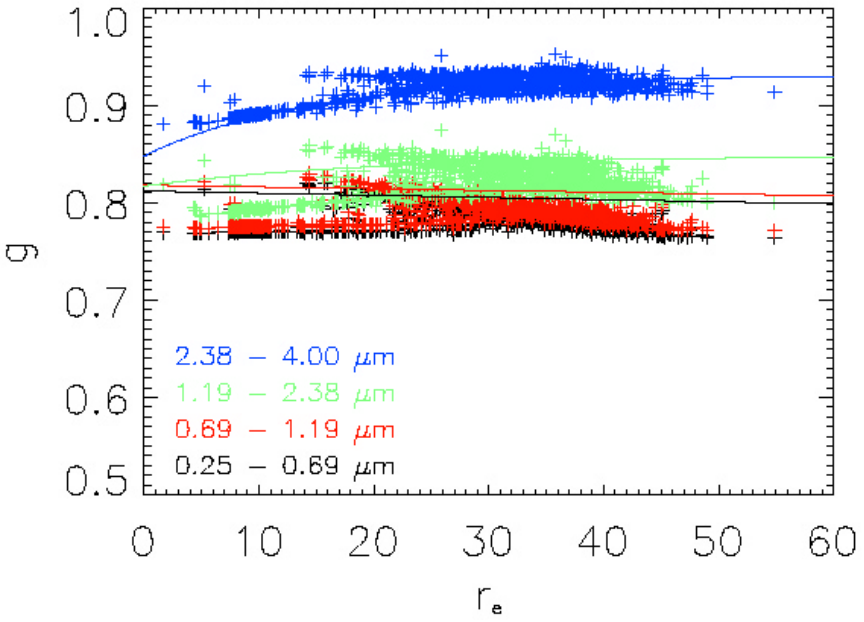

Figure 10. Mean asymmetry parameter for ice crystal distributions versus effective radius computed following Fu's (1996) definition. Solid lines represent fits for g versus r_e derived for CEPEX data that should represent behavior at TWP site.

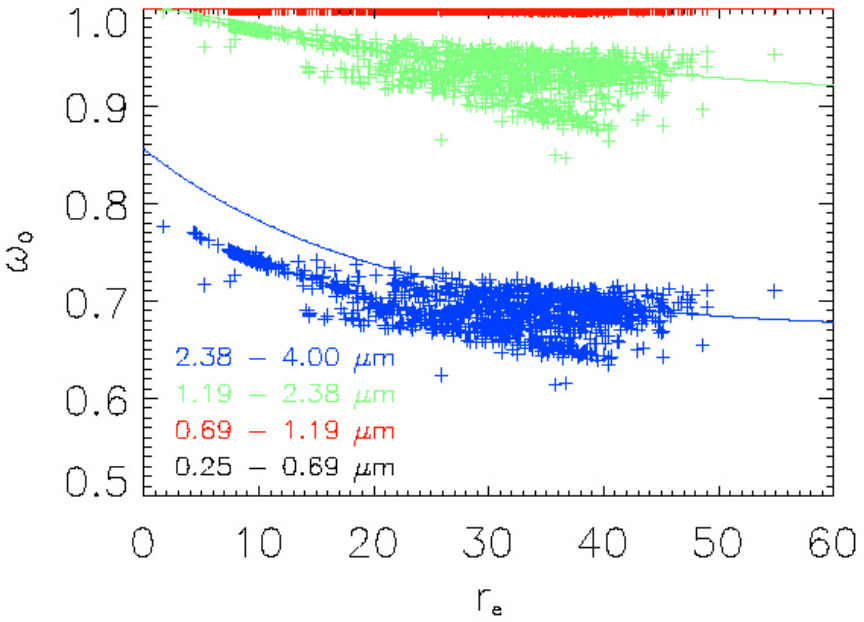

Figure 11. As in Figure 10, except for mean single-scatter albedo.

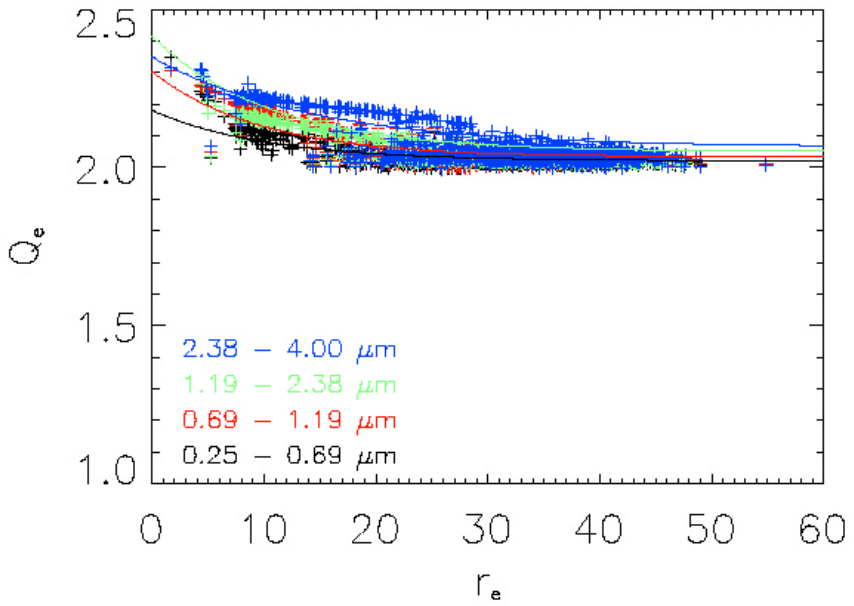

Figure 12. As in Figure 10, except for mean extinction efficiency.